Methods

Cell Culture

Human lung embryonic WI-38 fibroblasts (21 population doublings, PDs) obtained from the American Type Culture Collection were maintained and subcultured to 28 PDs in MEM (Gibco) supplemented with 10% FBS (Hyclone), 2 mM glutamine and 200 units/ml penicillin in a 37°C, 5% CO_2 incubator. For functional experiments, cells were plated at $1\times10^4/cm^2$ and cultured for 10 h on coverslips coated with 5 μg/ml fibronectin (Sigma).

Calcium Imaging

WI-38 cells were loaded with fluo-4 AM (5 μM) alone or in combination with fura-red AM (5 μM) for 6 min at 37°C, rinsed twice, and then bathed in Hepes-buffered saline solution containing (in mM): 134 NaCl, 5.4 KCl, 1.0 $MgSO_4$, 1.0 NaH_2PO_4, 1.8 $CaCl_2$, 20 Hepes, and 5 D-glucose (pH 7.4) with 1% FBS, unless otherwise specified. Cells were placed in a 37°C heated chamber (Zeiss S-Type incubator) and imaged on a Zeiss LSM 510 confocal microscope with a 40× oil objective (NA 1.3) at radial and axial resolutions of 0.4 and 1.0 μm, respectively. For ratiometric imaging, cells were excited at 488 nm, emission was detected at 505–550 nm (fluo-4 signal) and >633 nm (fura-red signal), and a DIC transmission image was acquired simultaneously. For migration path analysis and calcium flicker signal mass measurement, 300-600 time-lapse images were acquired at 6 s intervals. High resolution linescan imaging of calcium flickers was performed at 3 ms per linescan.

PCR

Total RNA was isolated from 28PDs WI-38 fibroblasts with TRI Reagent (Sigma) and converted to cDNA by using M-MLV reverse transcriptase (Promega). Quantitative RT-PCR reactions were carried out using these cDNAs in an iQ5 real-time PCR detection system (BioRad). Results were read out using iQ5 optical system software. All samples showing primer dimer formation or spurious, non-specific peaks, as indicated by the dissociation curve, were excluded from analysis. The primers are shown in supplementary Table 1.

RNA Interference

RNAi sequences for IP_3R isoforms and TRP channels were designed using RNAi Designer (http://www.invitrogen.com/rnai) (supplementary Table 2). Each scrambled control was designed corresponding to first duplex of siRNA. Briefly, corresponding siRNA duplexes were synthesized (GenePharma, Shanghai or Invitrogen, USA) and transfected into cells with Lipofectamine RNAiMax (Invitrogen) according to the manufacturer's recommendations. Western blotting or functional studies were carried out 72 h after transfection.

Western Blotting

Total protein extracted from WI-38 cells with siRNA treatment was separated on 4-12% NuPAGE Novex Bis-Tris gels (Invitrogen) and transferred to PVDF membranes (Millipore). After blocking for 1 h with 5% nonfat dry milk, the PVDF membrane was probed with primary antibody (anti-IP_3R2 was a gift

from Ju Chen at UCSD; anti-IP_3R3 from Santa Cruz; anti-tubulin from Sigma; anti-TRPC6 from Millipore; anti-TRPV2 from ABR; anti-TRPP2 and anti-TRPM7 from Abcam) for 2 h at room temperature, and then secondary antibody (IRDye-conjugated anti-mouse, anti-rabbit and anti-goat IgG from LI-COR) for 1 h at room temperature. Immunoblots were detected using the Odyssey imaging system.

Cell Migration Analysis

Fibroblasts with an overt leading lamella and a thin trailing edge were selected for migration analysis. The outer boundary of the cell was extracted from the respective fluorescence image for calculation of its centre of gravity. The centres of consecutive images (6 s apart) defined the trajectory of cell movement. Migration speed was calculated as the average displacement per min during 30 min. Directional persistence (D/T ratio) was calculated as the ratio between the linear displacement and the total length of the trajectory during 30 min.

To establish a PDGF-BB (PeproTech) gradient perpendicular to the long axis of a polarized migrating fibroblast, a 5 μm internal diameter, PDGF-BB-containing (3 nM) micropipette was placed ~150 μm away from one side of the cell. By visualisation of sulfurhodamine fluorescence under similar conditions, we estimated an average PDGF concentration of 1 nM and an edge-to-edge difference of 0.4 nM across the leading lamella (~40 μm).

Chemotaxis Assay

24–well Transwell plates with inserts containing 8 μm pores in a polycarbonate membrane (Corning) were used for chemotaxis assays. Briefly, the outer wells contained 600 μL MEM containing 1% FBS with PDGF-BB (0.8 nM) as chemoattractant. Approximately 8×10^3 overnight-starved (1% FBS) WI-38 fibroblasts in 100 μL PDGF-BB-free MEM containing 1% FBS and the designated drug were added to each insert. In the chemokinesis control group, PDGF-BB (0.8 nM) was also added to abolish the concentration gradient. The Transwell plate was then incubated for 12 h in a 37°C, 5% CO_2 incubator before assay.

For assay, the inserts were loaded with 5 μM calcein AM for 10 min and then fixed immediately with 3% formaldehyde for 10 min. Cells in inserts were cleared and those under the lower surface of the polycarbonate membrane were imaged and analysed.

Application of Mechanical Forces

Shear stress was locally applied by a gentle jet flow (4 cm H_2O pressure) *via* a patch pipette (10 μm internal diameter) ~80 μm from the front of migrating fibroblasts. Note that the jet flow used in local drug delivery (1 cm H_2O pressure, ~120 μm placement, pipette with 5 μm internal diameter) did not alter calcium flicker activity (n = 4).

Recording SACC Currents and Imaging Local Calcium Influx

The cell-attached patch-clamp technique, using an EPC-7 amplifier (Germany), was applied to fibroblasts preloaded with the calcium indicator,

fluo-4 AM. The patch pipette (2-3 MΩ) solution contained (in mM): NaCl 140, KCl 5.4, $MgCl_2$ 1.0, Hepes 20, and $CaCl_2$ 1.8 (pH 7.4, adjusted with NaOH). To activate SACCs, mechanical suction of ~40 mm Hg was applied *via* a syringe connected to the patch pipette while the patch membrane was held 80 mV more negative than the resting membrane potential to enhance Ca^{2+} entry. The single-channel currents were filtered at 3 kHz and digitised at 5 kHz with pClamp 6.0 software. Linescan images of local calcium immediately beneath the patch membrane were acquired simultaneously at 3 ms resolution.

Data Analysis

Digital image processing used IDL software (Research Systems) and custom-devised computer algorithms. Statistical data are expressed as mean ± s.e.m. Student's *t*-test and paired *t*-test were applied when appropriate. A P value less than 0.05 was considered statistically significant.

Supplementary Figure 1

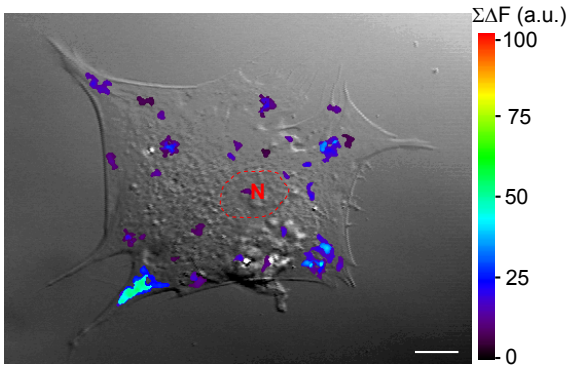

Calcium flickers in a stationary fibroblast.

Experimental conditions as in Fig. 1a, except for selecting stationary WI-38 fibroblasts (24 h serum-starved) without polarisation. Local calcium increase (ΣΔF) extracted from 30 consecutive image frames captured at 6 s intervals shown as overlay on a DIC transmission image of the cell. "N" marks the nuclear region. Note that calcium flicker activity lacked directional polarisation across the cell. Scale bar: 10 μm. Similar results were obtained in 5 stationary cells.

Supplementary Figure 2

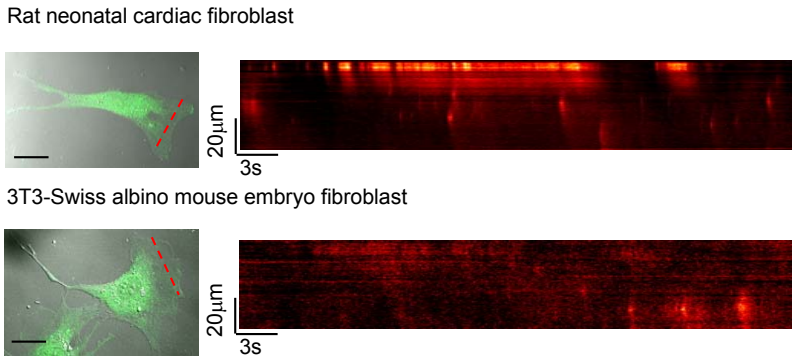

Calcium flickers in other fibroblasts.

Calcium flickers similar to those in human WI-38 fibroblasts were detected in the lamella of migrating fibroblasts from rat neonatal cardiac fibroblasts (upper panels) and mouse 3T3-Swiss albino embryo fibroblasts (lower panels). The left panels show overlays of the transmission image (black-and-white) and the fluo-4 image (green). Dashed lines show the scanning position. Scale bar: 20 μm.

Supplementary Figure 3

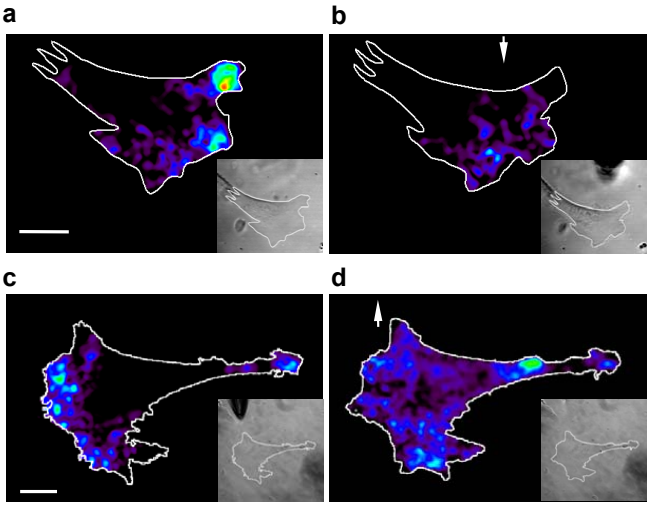

Calcium flickers responding to local manipulation of the substrate tension.

WI-38 fibroblasts were cultured on a flexible substrate. A needle tip on the side near the front of a cell pushed or pulled the substrate horizontally. Local calcium increases measured by fluo-4 were summed over 32 consecutive images acquired at 0.8 s intervals. **a-b,** calcium flicker activity before (a) and after (b) the tip pushed the substrate toward the cell to relax the substrate tension. Similar results were obtained in another 3 cells. **c-d,** calcium flicker activity before (c) and after (d) pulling the substrate away from the cell to stretch the substrate. Similar results were obtained in other 4 cells. Scale bar: 20 μm. Arrows show the directional motion of the tip and insets show the transmission image; in some images, the needle tip is seen on the upper side of the lamella.

Supplementary Figure 4

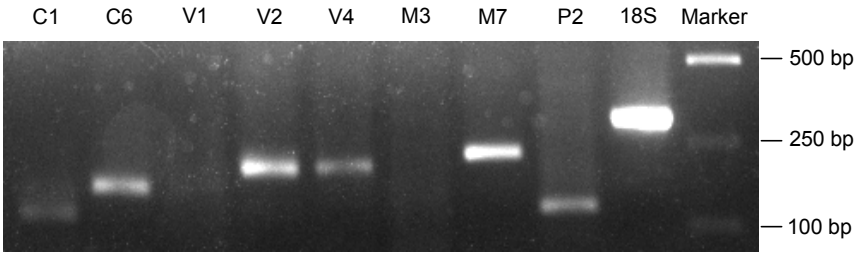

PCR analysis of expression of mechanically sensitive TRP channels in WI-38 fibroblasts.

C1, TRPC1; C6, TRPC6; V1, TRPV1; V2, TRPV2; V4, TRPV4; M3, TRPM3; M7, TRPM7 ; P2, TRPP2. See Supplementary Table 1 for primer sequences. 18S denotes 18S rRNA.

Supplementary Figure 5

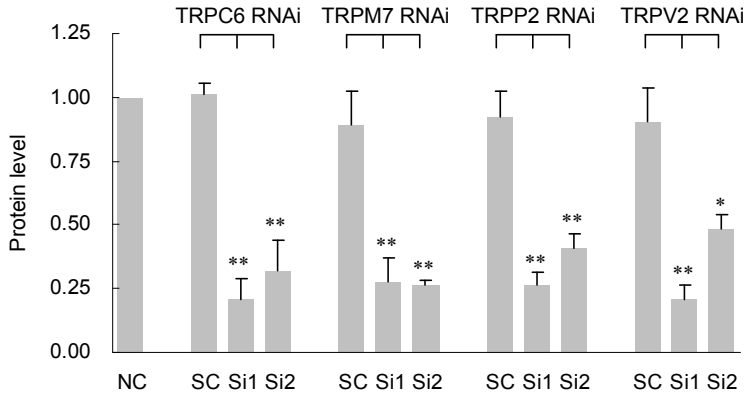

Statistics of TRP channel knockdown.

Representative TRP channel knockdown efficiency was assayed by western blotting. Error bars represent s.e.m.; n=3-5; *p < 0.05; **p < 0.01 *vs*. respective scrambled control RNA (SC).

Supplementary Figure 6

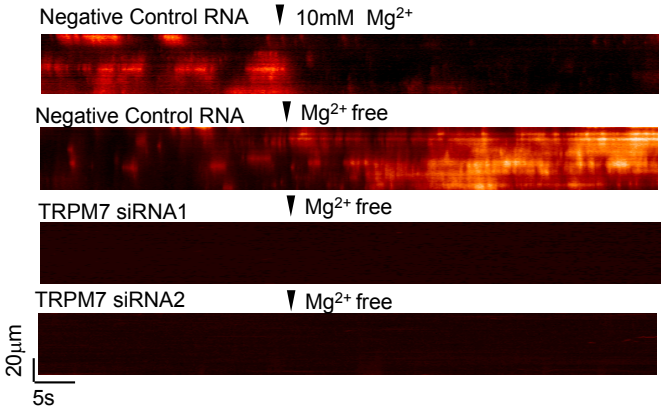

Mg^{2+} modulation of calcium flickers in the lamella of WI-38 fibroblasts.

Removing extracellular Mg^{2+} immediately enhanced the flicker activity, while elevation of extracellular Mg^{2+} rapidly inhibited calcium flickers. TRPM7 knockdown fibroblasts remained largely quiescent upon removal of extracellular Mg^{2+}.

Supplementary Figure 7

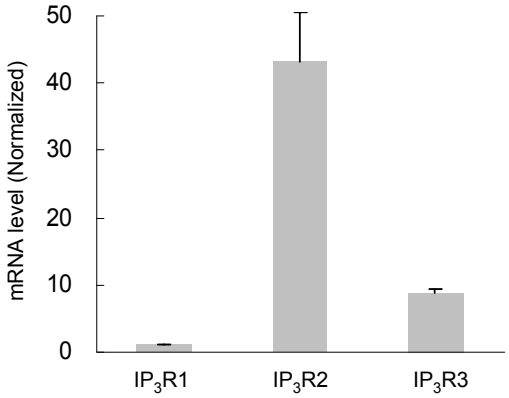

Quantitative RT-PCR for IP_3R isoform expression in WI-38 fibroblasts.

The mRNA expression of IP_3R isoforms was normalised to that of 18S rRNA. The IP_3R isoform mRNA level is expressed as fold-change over IP_3R1. Error bars represent s.e.m.(n=3-5).

Supplementary Figure 8

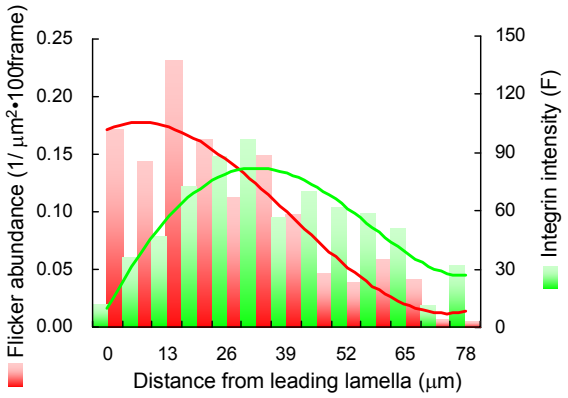

Axial distribution of calcium flickers (red) and FAs (green) in leading lamella.

Smooth curves show multinomial fits to the data. Notice the subtle difference that higher flicker activity was found at the leading protrusions of lamella with fewer FAs. This is perhaps because membrane tension at the foremost front can be augmented by a hydrostatic protrusive force generated from cortical acto-myosin contraction[31].

Supplementary Figure 9

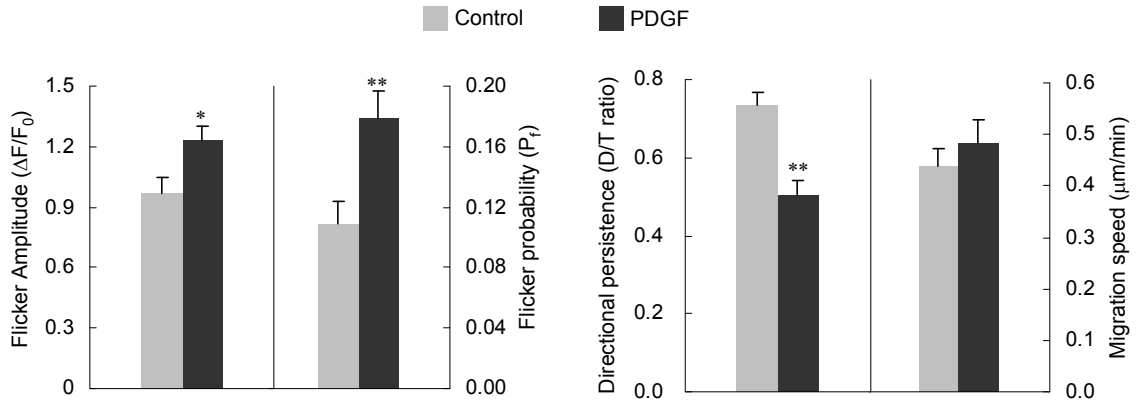

Effects of uniform PDGF on characteristics of calcium flickers and migration.

Flicker amplitude and probability (P_f) were calculated from linescan images (control group, n = 12; PDGF group, n = 11). Two parameters to describe cell migration, migration speed and directional persistence (D/T ratio) were analysed from 30-min time-lapse images (control group, n = 27; PDGF group, n = 20). Error bars represent s.e.m.; *p < 0.05 *vs.* control; **p < 0.01 *vs.* control. Note that bathing the cell with uniform PDGF-BB (0.8 nM) increased both flicker amplitude and probability. Concomitantly, PDGF reduced directional persistence, indicating enhanced turning behaviour. In the population of cells already undergoing migration, PDGF did not significantly alter the migration speed, as if flicker-promoted turning masked a possible flicker enhancement of migration speed. Consistent with this idea, the population of migrating cells increased from 21% (22 of 106 cells) in control to 55% (52 of 93 cells) in PDGF.

Supplementary Figure 10

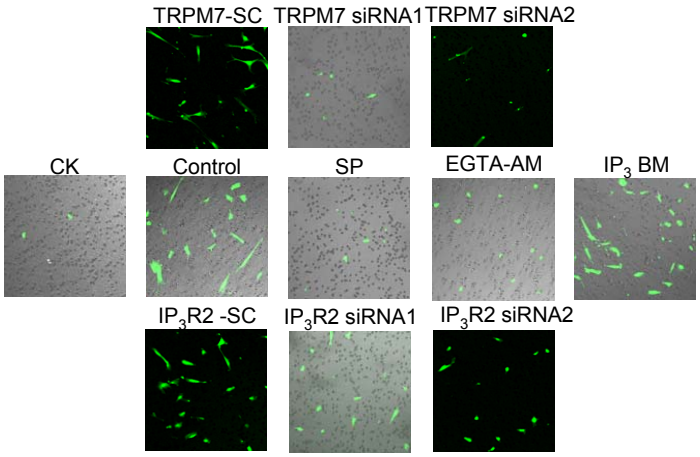

Representative results of chemotaxis in Transwell plates with different treatments.

Each panel shows transwell migrated cells in a 0.65×0.65 mm area. See Fig 5d for statistics.

Supplementary Figure 11

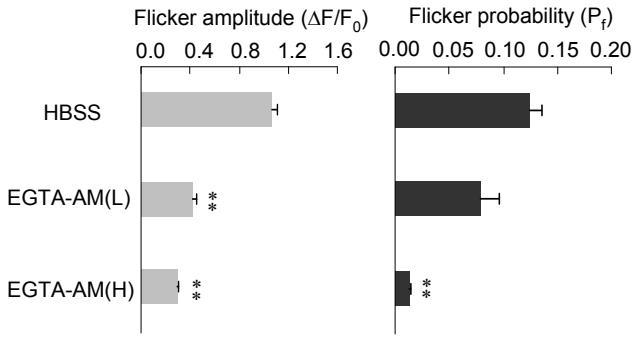

Effects of EGTA buffering on calcium flicker characteristics.

EGTA–AM (L) and EGTA–AM (H): membrane-permeable ester form of EGTA at low (L: 2 μM, 10 min, n = 8) and high doses (H: 20 μM, 10 min, n = 7). Error bars represent s.e.m, **p < 0.01 *vs.* HBSS.

Supplementary Table 1:Primer sequences for PCR

Name	Sequence（from 5` to 3`）
TRPC1	Forward: TTCAACATCATTCCCTCACC Reverse: GTTTCAAATTCCTCCATTCC
TRPC6	Forward: AGAATGCCACTCACTCAACG Reverse: TCCACAATCCGAACATAACC
TRPV1	Forward: ATGGCAAGGACGACTACCG Reverse: AGGGCAAAGTTCTTCCAGTGTC
TRPV2	Forward: GATGCTGACCGTTGGCACT Reverse: GCTGGACGGGCACATAGTT
TRPV4	Forward: GGCACCTATCGTCACCACTC Reverse: TCCTCATCAGTTAGGCGTTTC
TRPM3	Forward: TTATCGCTGCAACTACACGC Reverse: AATGTCCACCTCTTCTTCACG
TRPM7	Forward: GCACCATCTTGGACTCTT Reverse: GAAATTGCCTTCACTTGTA
TRPP2	Forward: GCATTCCATCGGCAGCATAG Reverse: TCACGACCCAGCCTTTCATC
18s rRNA	Forward: GGAAGGGCACCACCAGGAGT Reverse: TGCAGCCCCGGACATCTAAG
IP_3R1	Forward: CCACAGACGCAGTGCTACTCA Reverse: TTGCCATACTGGATTACGGT
IP_3R2	Forward: AACCTCATGGCAAAGCTATCA Reverse: CGAACAGGCACCACGGAC
IP_3R3	Forward: CCTGGAAATCCTTCAGTTCAT Reverse: CATGTTGGCAGTGGTAGAGTC

Supplementary Table 2: Oligos for siRNA

Name	Sense oligos（from 5`to 3`）
TRPC6	Scrambled control: GGUAGCACGACAGAUUCAA siRNA1: GGUUUACGACAGCAGACAA siRNA2: GGAAAUUUGCAAGGGCCAA
TRPV2	Scrambled control: GCUUUCGUCCUAAUUCCUU siRNA1: GCUUCCUUCUGAUCUACUU siRNA2: CCUUAAGGACGGAGUCAAU
TRPM7	Scrambled control: CCUAAGUCACGUACACCUU siRNA1: CCUCAUGAAGCACCAUCUU siRNA2: AACAUCAGACGAACAGAAUUAGUUG
TRPP2	Scrambled control: GGACGACACGUAACAAGUU siRNA1: GGAAACAGCUGCACAAGUU siRNA2: CCAUAAAGCUUUGGUCAAA
Negative Control	UUCUCCGAACGUGUCACGU
IP_3R2	Scrambled control: GGUACCGAUAACCUACCUU siRNA1: GGUACCAGCUAAACCUCUU siRNA2: GGGCCUGCUUGGGAUUACAGAAAUA
IP_3R3	Scrambled control: GGGUGAAAGUUAAUCACAA siRNA1: GGGACAAGUUUGAUAACAA siRNA2: CCUACCUGCUGUCUGUCUU

Supplementary Note

Reference

31. Charras, G. T., Yarrow, J. C., Horton, M. A., Mahadevan, L. & Mitchison, T. J. Non-equilibration of hydrostatic pressure in blebbing cells. *Nature* **435**, 365-369 (2005).